Realization of a Magnetically Guided Atomic Beam in the Collisional Regime

T. Lahaye, J. M. Vogels, K. J. Günter, Z. Wang, J. Dalibard, and D. Guéry-Odelin
Laboratoire Kastler Brossel, 24 rue Lhomond, F-75231 Paris Cedex 05, France*
(Received 30 April 2004; published 26 August 2004)

We describe the realization of a magnetically guided beam of cold rubidium atoms, with a flux of 7×10^9 atoms/s, a temperature of 400 μK, and a mean velocity of 1 m/s. The rate of elastic collisions within the beam is sufficient to ensure thermalization. We show that the evaporation induced by a radio-frequency wave leads to appreciable cooling and an increase in the phase space density. We discuss the perspectives to reach the quantum degenerate regime using evaporative cooling.

DOI: 10.1103/PhysRevLett.93.093003 PACS numbers: 32.80.Pj, 03.75.Pp

The recent realization of slow atom sources using laser cooling methods has constituted a major advance for many applications in metrology and matter wave interferometry [1]. The possibility to complement laser cooling by forced evaporation has led to even colder and denser atomic gases, and has culminated with the observation of Bose-Einstein condensation [2] and pulsed "atom lasers" extracted from the condensate [3]. These advances allow us in principle to build a continuous and coherent source of matter waves which would be the equivalent of a monochromatic laser. It should lead to unprecedented performances in terms of focalization or collimation, and provide a unique tool for developments in atom manipulation and precision measurements.

Two paths have been considered to reach the goal of a continuous and coherent source of atoms ("cw atom laser"). The first possibility [4] consists in using the "standard" condensation procedure to periodically replenish with new condensates a gas sample held in an optical dipole trap. The second possibility, investigated here, consists in transposing the evaporative cooling method to a guided atomic beam [5]. As the beam progresses in a magnetic guide [6,7], most energetic atoms are removed and remaining particles thermalize at a lower temperature and a larger density, so that the beam can eventually reach the degenerate regime. This method should allow for a large flux, since it consists in a parallel implementation of the various steps to condensation. This gain in flux can constitute a major advantage for applications.

To implement this method, the initial atomic beam needs to be deeply in the collisional regime. The number N_{col} of elastic collisions undergone by each atom as it travels along the guide must be large compared to unity, to provide the thermalization required for evaporative cooling. Such beams were so far not available. In this Letter we report on the realization of a rubidium atomic beam in the collisional regime, with $N_{\mathrm{col}} \sim 8$. It propagates in a 4.5 m long magnetic guide with a mean velocity of 1 m/s. We also demonstrate a first step of evaporative cooling, and show that the measured increase in phase space density is in good agreement with expectations. Finally, we discuss possible improvements of the current setup which should allow us to reach the degenerate regime.

Figure 1 shows the layout of our experimental setup, composed of three main parts lying in the xy horizontal plane: the Zeeman slower along the y axis, the magneto-optical trap (MOT), and the magnetic guide along the x axis. The Zeeman slower [8] consists of a 1.1 m long tapered solenoid in which atoms emerging from an oven are decelerated by resonant radiation pressure. It delivers a flux of 2×10^{11} s^{-1} ^{87}Rb atoms, with a velocity of 20 m/s. The slow atoms are captured in a MOT formed by three pairs of counterpropagating beams. One pair of beams is aligned with the vertical (z) axis, and the other two pairs are along the directions $\boldsymbol{e}_x \pm \boldsymbol{e}_y$. Each trapping beam has a circular profile, with a $1/e^2$ radius of 17 mm and a power of 15 mW.

The entrance of the magnetic guide is located 4.6 cm away from the MOT center. The guide, which is placed inside the vacuum system, consists of four parallel,

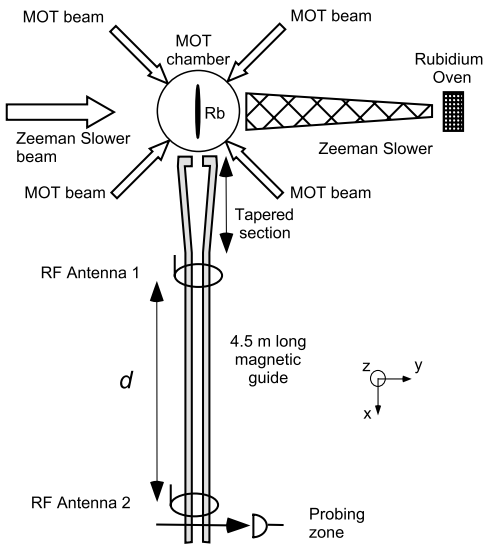

FIG. 1. Top view of the setup. The atoms emerging from the oven are slowed down by radiation pressure, captured in the magneto-optical trap, and launched into the magnetic guide.

 0031-9007/04/93(9)/093003(4)$22.50

water-cooled copper tubes, in which we run a current I up to 400 A. Unless otherwise stated, parameters and results given below correspond to $I = 240$ A. The entrance of the guide consists of a ring shaped metal part, used for the recombination of the electric and cooling water circuits [7]. At this location the distance between the centers of adjacent tubes is 14 mm, resulting in a gradient of $b'_0 = 200$ G/cm. The first 40 cm of the guide form a tapered section, obtained by reducing progressively the distance between the tubes to 8 mm. This results in an increase of the trapping gradient to $b'_1 = 600$ G/cm. The guide provides a confinement of the atoms of magnetic moment μ with a linear potential $\mu b'(y^2 + z^2)^{1/2}$ [9].

To optimize the transfer from the MOT into the magnetic guide, we operate in pulsed mode [10], with a duration of $t_{\rm seq} = 283$ ms per sequence. In the first 140 ms we capture 3×10^9 atoms in the MOT. All beams are set at frequency ω_L, corresponding to a detuning $\Delta = \omega_L - \omega_A = -3\Gamma$, where Γ is the natural width of the $5P_{3/2}$ excited state and ω_A the atomic resonance frequency. The MOT magnetic gradients are $b'_x = 0.6$ G/cm, $b'_y = 5.4$ G/cm, and $b'_z = -6$ G/cm. The MOT is thus cigar shaped, with a $1/\sqrt{e}$ radius of 1.4 mm and a length of 35 mm, the long axis being along the magnetic guide direction.

The MOT magnetic field is then turned off and a 3 ms launching phase occurs. The detunings of the horizontal beams are shifted by $\pm k_L v/\sqrt{2}$ with respect to the detuning Δ of the vertical beams, where $k_L = \omega_L/c$. This forms a moving molasses that sets the atoms in motion at velocity $v = 1.1$ m/s towards the magnetic guide [11]. The detuning Δ is ramped to -10Γ, which reduces the temperature of the gas to $T_0 = 40$ μK in the frame moving at velocity v.

The final phase of the sequence consists of (i) optical pumping of the moving atoms into the weak-field-seeking ground state $|F = 1, m_F = -1\rangle$, and (ii) magnetic preguiding of the atom cloud. The preguiding is provided by a two-dimensional (yz) quadrupole magnetic field with a gradient $b'_2 = 65$ G/cm generated by four elongated coils (not shown in Fig. 1), located around the MOT chamber. It prevents the atom cloud from expanding during its flight towards the entrance of the magnetic guide. During the preguiding phase we also apply at the MOT location a 56 G bias field along x to match the oscillation frequency in the preguide with the cloud parameters. The overall efficiency of the pumping + preguiding process is 60% so that each packet loaded into the guide contains $N_{\rm load} \sim 2 \times 10^9$ atoms. We measure the atom number and mean velocity by monitoring the absorption of a probe beam at the end of the guide. Losses due to collisions with residual gas are negligible.

We estimate numerically the influence of the rapid variation of the magnetic gradient from b'_2 to b'_0 at the entrance in the main guide by analyzing single particle trajectories. The cloud is compressed to a final transverse radius $r_0 = 400$ μm and an energy per atom of $k_B \times 500$ μK in the moving frame. In the subsequent propagation into the tapered section of the guide, the gradient increases to b'_1 and the bias field decreases to 0 [9]. It leads to a further, quasiadiabatic, compression of the cloud, and the energy per atom in the moving frame raises to $E = k_B \times 1400$ μK. Assuming thermalization via elastic collisions, we find using the virial theorem that this energy is shared as $3k_BT_1/2$ for the kinetic energy and $2k_BT_1$ for the potential energy of the transverse linear confinement, with $T_1 = 400$ μK. This estimate for T_1 agrees well with measurement as we see below.

The next capture + launch sequence starts 140 ms after the beginning of the preguiding phase, so that the atom packet has moved ~14 cm away from the MOT center and is now well inside the main guide. Owing to this protocol, the light scattered from the MOT during the preparation of a packet does not produce detectable losses on the previous packet. Figure 2 shows the signal detected for different numbers of launches. The area of the signal scales linearly with this number.

To generate a continuous beam we repeat the sequence with a cycling rate of $t_{\rm seq}^{-1} = 3.5$ Hz. For $T = 400$ μK the packets overlap after a propagation of 60 cm. The flux is $\phi = N_{\rm load} t_{\rm seq}^{-1} = 7(\pm 2) \times 10^9$ atoms/s. The deviation δH of the guide from a horizontal plane is <1 cm over the 4.5 m length. It induces small changes of the mean velocity and temperature of the beam [12]: $\delta v/v = g\delta H/v^2$ ($<8\%$) and $\delta T/T = (2/7)\delta v/v$ ($<3\%$), respectively, where g is the acceleration due to gravity.

We now turn to the characterization of the beam and the demonstration that the collisional regime has been reached. For this study we use radio-frequency (rf) antennas located along the guide, which generate an oscillating magnetic field at frequency ν. An antenna flips the magnetic moment of the atoms passing at a distance $r_{\rm e} = h\nu/(\mu b')$ from the x axis [13]. For an atom of mass m, with transverse energy E and angular momentum L along the x axis, the evaporation criterion $r = r_{\rm e}$ is fulfilled at some points of the atom trajectory if

$$E \geq \frac{L^2}{2mr_{\rm e}^2} + \mu b' r_{\rm e}. \qquad (1)$$

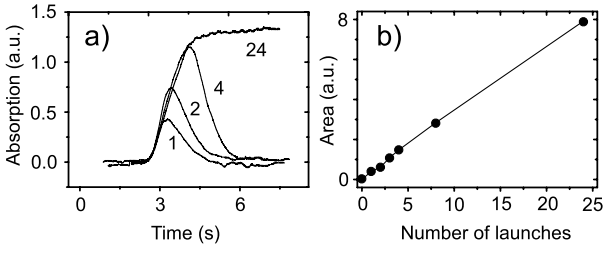

FIG. 2. (a) Absorption signal at the end of the guide for 1, 2, 4, and 24 launches. The time origin corresponds to the launching of the first packet. (b) Number of atoms (area of the absorption signal) as a function of the number of launches.

An antenna, whose range is ~20 cm, constitutes a local probe of the (E, L) distribution at the scale of the guide.

The temperature in the guide is deduced from the variation of the fraction f of remaining atoms after the antenna. Qualitatively one expects that f is minimum when $h\nu \sim k_B T$, and that $f \sim 1$ when $h\nu \ll k_B T$ or $h\nu \gg k_B T$. Indeed, for small ν, few atoms have a sufficiently low angular momentum to be evaporated. For large ν the evaporative loss is negligible because of the exponential decay of the energy distribution. For a given power law dependence of the confining potential, the fraction f is a "universal function" of the dimensionless parameter $\eta = h\nu/(k_B T)$. For a quadratic confinement one finds [14] $f(\eta) = 1 - \sqrt{\pi\eta}e^{-\eta}$. For our linear confinement we could not obtain a simple analytical formula, and we used a Monte Carlo determination of $f(\eta)$. The result is fitted to better than 2% by the expression

$$f(\eta) = 1 - A\eta^B e^{-C\eta} \tag{2}$$

with $A = 1.65$, $B = 1.13$, and $C = 0.92$.

A typical measurement of f is given in Fig. 3(a), together with a fit using (2). The transverse temperature corresponding to the best fit is $384(\pm 13)$ μK, in good agreement with the expected temperature given above. For the fit we allow the coefficient A in (2) to vary, to account for a possible uncomplete efficiency of the evaporation process. For the data of Fig. 3(a), the efficiency is better than 90%. We have checked for all our data that allowing A to vary changes the fitted temperatures by less than 5% from the results obtained with $A = 1.65$.

The thermal equilibrium assumption used above is valid only if a sufficient number of elastic collisions (at least a few per atom) has occurred in the guide. To investigate whether the collisional regime has been reached, we turn to a two-antenna experiment [Fig. 3(b)]. These antennas are located, respectively, $d_1 = 1$ m and $d_2 = 4$ m after the entrance of the guide. The frequency ν_1 of the first antenna is fixed at $\nu_1 = 24$ MHz, which corresponds to $\eta_1 = h\nu_1/(k_B T_1) = 3$, where T_1 is the temperature deduced from the analysis of Fig. 3(a). This antenna evaporates the atoms fulfilling (1), thus producing an out-of-equilibrium distribution. We measure the function $f(\eta_2)$ with the second antenna, and check whether a thermal distribution is recovered during the propagation from d_1 to d_2. The result for $f(\eta_2)$ in Fig. 3(b) shows that this is the case, with $T_2 = 281(\pm 8)$ μK. The fact that $T_2 < T_1$ is a clear demonstration of evaporative cooling of the beam by the first antenna.

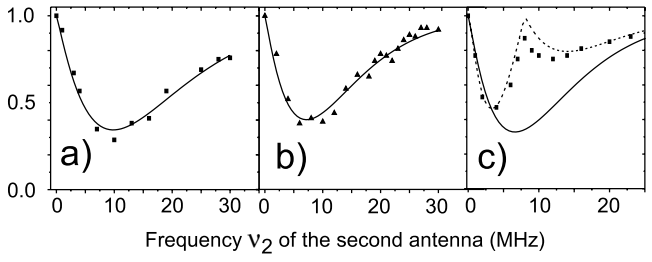

FIG. 3. Experiment with two antennas separated by a distance d: remaining fraction after the second antenna, with the first antenna set at a fixed value ν_1. (a) Antenna one off, flux ϕ, $b_1' = 600$ G/cm, and $d = 3$ m. Using (2) as a fit function (solid line), we find $T_1 = 384(\pm 13)$ μK. (b) $\nu_1 = 24$ MHz with the same conditions as for (a). The fit gives $T_2 = 281(\pm 8)$ μK, indicating a significant cooling. (c) $\nu_1 = 8$ MHz and reduced number of collisions between antennas: flux $\phi/3$, $b_1' = 400$ G/cm, and $d = 0.85$ m. The dotted line is the prediction for the collisionless regime. The solid line is the result expected if thermalization had occurred.

We have investigated the thermalization process as a function of η_1 (Fig. 4). For $\eta_1 \lesssim 1.25$ the evaporated atoms have less energy than average, leading to heating $(T_2 > T_1)$. Cooling is observed in the opposite case $\eta_1 \gtrsim 1.25$. The continuous line in Fig. 4 is the theoretical prediction assuming full thermalization between d_1 and d_2. It is in excellent agreement with the experimental results. The phase space density on axis is $n_0\lambda_{\mathrm{dB}}^3$, where $\lambda_{\mathrm{dB}} \propto T^{-1/2}$ is the de Broglie wavelength and $n_0 \propto \phi/T^2$ is the central density for a linear transverse confinement. For $\eta_1 = 3$ [Fig. 3(b)] we measure a decrease of flux and temperature by 36% and 27%, respectively. This corresponds to an *increase* in phase space by a factor $1.92(\pm 0.15)$, to be compared with the expected gain of 1.90. This transverse evaporation mechanism is thus well suited to bring the beam in the degenerate regime.

For the sake of completeness we performed a similar study with the beam in the collisionless regime. This regime can be reached by reducing the flux and/or weakening the confinement. To keep a reasonable signal to noise ratio we divided the flux only by a factor of 3. Therefore, to reach the collisionless regime we also operated the magnetic guide at a lower current (160 A). The measured temperature is in this case $T_1 = 230(\pm 6)$ μK. To minimize the thermalization process between the

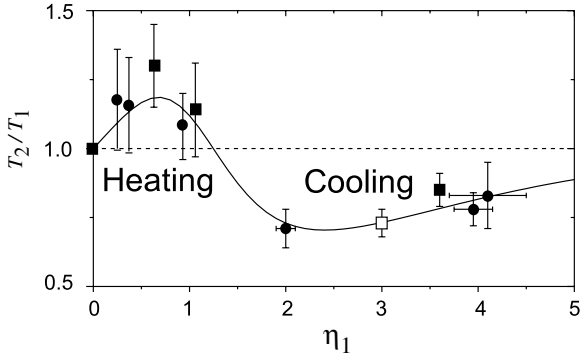

FIG. 4. Ratio T_2/T_1 between the temperature T_2 of the beam when the first antenna is set at ν_1 and the temperature T_1 of the beam in absence of evaporation, as a function of $\eta_1 = h\nu_1/(k_B T_1)$. The solid line is the theoretical prediction for a linear potential (no adjustable parameter). The open square corresponds to the data of Fig. 3(b). The squares (circles) have been obtained with $I = 240$ A (400 A).

antennas, we also reduced the distance $d_2 - d_1$ to 0.85 m. The result for $f(\eta_2)$ is shown in Fig. 3(c) for $\nu_1 = 8$ MHz. The dashed line gives the result expected in the collisionless regime. In this case the second antenna does not induce extra loss when $\nu_2 = \nu_1$ since no modification of the (E, L) distribution occurs between the two antennas. The measured $f(\eta_2)$ is in good agreement with this prediction. For comparison we also indicate in Fig. 3(c) the expected signal in case of a complete thermalization. It does not agree with our data, contrary to the large flux case [Fig. 3(b)].

To summarize, our guided beam is deeply in the collisional regime when operated at the maximum flux. The collision rate in the linear guide is $\gamma_c = n_0 \sigma \Delta v / \sqrt{\pi} = 2\ \mathrm{s}^{-1}$, where $n_0 = 2.8 \times 10^{10}\ \mathrm{cm}^{-3}$, $\sigma = 6.8 \times 10^{-12}\ \mathrm{cm}^2$ is the s-wave elastic cross section and $\Delta v = \sqrt{k_B T/m} = 19$ cm/s. This corresponds to $N_{\mathrm{col}} = 8$ collisions per atom along the whole guide. For the experiment of Fig. 3(b), taking into account the reduction of flux by the first antenna, we estimate that each atom undergoes three collisions between the two antennas. This is known to be the minimum value to ensure thermalization (see, e.g., [15]).

Finally, we discuss the possibility to use this device for producing a coherent continuous atomic wave. The current phase space density at the center of the beam is 2×10^{-8}. To reach degeneracy, we plan to use several antennas with decreasing frequencies. Operating all antennas at the same η, the cooling distance is minimized for $\eta \sim 4$. We need 40 antennas, each providing a phase space increase of 1.63. The expected output flux is $2 \times 10^{-4} \phi$ for a cooling distance of $\sim 100 v/\gamma_c$. To match this distance with the guide length, we have to increase the initial collision rate γ_c by 1 order of magnitude. A fraction of this gain can be obtained by slowing down the beam by gravity, using a tilted guide [12]. In addition, we plan to transpose to our elongated MOT the "dark spot" technique, which leads to a significant gain in terms of spatial density of the laser cooled atomic source [16]. A continuous coherent atomic beam will be a useful tool for the interferometric and metrology applications mentioned above, as well as for studies of fundamental issues, such as superfluidity in quasi-one-dimensional systems. Another challenge is the miniaturization of the setup, as recently performed for the production of standard Bose-Einstein condensates with "atom chips" [17].

We acknowledge stimulating discussions with the ENS laser cooling group. We thank A. Senger for his participation in the data acquisition. K. J. G. acknowledges support from the Marie Curie Host fund through Grant No. HPMT-CT-2000-00102. J. M. V. acknowledges support from the Research Training Network "Cold Quantum Gases" HPRN-CT-2000-00125. This work was partially supported by Région Ile-de-France, Délégation Générale de l'Armement, Bureau National de la Métrologie, Ministère de la Recherche, and Collège de France.

*Unité de Recherche de l'Ecole Normale Supérieure et de l'Université Pierre et Marie Curie, associée au CNRS.

[1] P. R. Berman, *Atom Interferometry* (Academic Press, London, 1997).
[2] C. J. Pethick and H. Smith, *Bose-Einstein Condensation in Dilute Gases* (Cambridge University Press, Cambridge, 2002); L. P. Pitaevskii and S. Stringari, *Bose-Einstein Condensation* (Clarendon Press, Oxford, 2003).
[3] K. Helmerson, D. Hutchinson, K. Burnett, and W. D. Phillips, Phys. World **12**, 31 (1999), and references therein.
[4] A. P. Chikkatur *et al.*, Science **296**, 2193 (2002).
[5] E. Mandonnet *et al.*, Eur. Phys. J. D **10**, 9 (2000).
[6] M. Key *et al.*, Phys. Rev. Lett. **84**, 1371 (2000); N. H. Dekker *et al.*, Phys. Rev. Lett. **84**, 1124 (2000); B. K. Teo and G. Raithel, Phys. Rev. A **63**, 031402 (2001); J. A. Sauer, M. D. Barrett, and M. S. Chapman, Phys. Rev. Lett. **87**, 270401 (2001).
[7] P. Cren *et al.*, Eur. Phys. J. D **20**, 107 (2002).
[8] H. J. Metcalf and P. van der Straten, *Laser Cooling and Trapping* (Springer-Verlag, New York, 1999).
[9] Strictly speaking, the magnetic field at the center of the guide does not vanish thanks to the x component of the Earth magnetic field, which prevents Majorana spin flips.
[10] J. M. Vogels *et al.*, cond-mat/0404560.
[11] A. Clairon, C. Salomon, S. Guellati, and W. D. Phillips, Europhys. Lett. **16**, 165 (1991).
[12] T. Lahaye, P. Cren, C. Roos, and D. Guéry-Odelin, Commun. Nonlinear Sci. Numer. Simul. **8**, 315 (2003).
[13] O. J. Luiten, M. W. Reynolds, and J. T. M. Walraven, Phys. Rev. A **53**, 381 (1996); W. Ketterle and N. J. van Druten, Adv. At. Mol. Opt. Phys. **37**, 181 (1996).
[14] C. Roos *et al.*, Laser Phys. **13**, 605 (2003).
[15] C. R. Monroe *et al.*, Phys. Rev. Lett. **70**, 414 (1993).
[16] W. Ketterle *et al.*, Phys. Rev. Lett. **70**, 2253 (1993).
[17] W. Hänsel, P. Hommelhoff, T. W. Hänsch, and J. Reichel, Nature (London) **413**, 498 (2001); H. Ott, J. Fortägh, G. Schlotterbeck, A. Grossmann, and C. Zimmermann, Phys. Rev. Lett. **87**, 230401 (2001); A. E. Leanhardt *et al.*, *ibid.* **89**, 040401 (2002); S. Schneider *et al.*, Phys. Rev. A **67**, 023612 (2003).